GENERALIZED CHAKRAVERTY–WAGNER DISTRIBUTION

R.D. VENGRENOVICH, B.V. IVANS'KYI, A.V. MOSKALYUK

Yu. Fed'kovich Chernivtsi National University
(2, Kotsyubinskyi Str., Chernivtsi 58012, Ukraine)

UDC 539.3

A mechanism of the Ostwald ripening of islands in thin films and heterostructures under the simultaneous action of the diffusion and Wagner growth mechanisms is proposed. The island size distribution function and the corresponding time dependences for the average (critical) and maximal dimensions of islands are calculated. The comparison of the experimental histograms with the calculated curves confirms the possibility of practical realization of the proposed growth mechanism in the process of Ostwald ripening.

1. Introduction

The phase structure and dispersion (particle size distribution) at late stages of the decay of an oversaturated solid solution, i.e. the Ostwald ripening (OR) stage [1], are determined by the mechanisms of mass transfer between structural components. If the growth of particles of a different phase is limited by the coefficient of volume or matrix diffusion D_v, then the average size of precipitates (particles, clusters) $\langle r\rangle$ changes in time as $t^{1/3}$, whereas the particle size distribution is described by the Lifshitz–Slyozov distribution [2, 3]. In the case where the growth of clusters is controlled by processes taking place at the "particle–matrix" interface, i.e. by the kinetic coefficient β, $\langle r\rangle$ varies as $t^{1/2}$, while the size distribution corresponds to the Wagner distribution [4]. In the case of the simultaneous action of these two mechanisms of growth proposed in [2–4], the dispersion of precipitates is described by the generalized Lifshitz–Slyozov–Wagner distribution [5].

Works [2–4] represent the basis of the Ostwald ripening theory also called the Lifshitz-Slyozov-Wagner theory or simply the LSW theory. In the framework of this theory, a number of other problems related to the investigation of OR under the conditions of the diffusion along grain boundaries [6,7] and dislocation tubes [8–13] were later solved. The LSW theory is also used for the analysis of dissipative structures in nonequilibrium semiconductor systems [14,15].

However, of special interest is the extension of the LSW theory to surface dispersed systems and particularly island films. It is especially urgent today taking the development of nanotechnologies and the production of nanostructures into account [16–22]. In particular, semiconductor heterostructures with quantum dots obtained in the process of self-organization in the Stranski–Krastanow mode [23,24] are of important practical use.

Chakraverty for the first time applied the LSW theory to the description of the evolution of a structure of discrete films consisting of separate islands (clusters) and having a form of spherical segments (Fig. 1) [35].

In the Chakraverty model, a film consists of separate dome-shaped islands (Fig.1) statistically uniformly distributed over the substrate surface in the oversaturated sea (solution) of atoms absorbed by the substrate (adatoms). One can see from Fig. 1 that the dome-shaped clusters in the form of segments represent a part of the sphere with the radius R_C and the contact angle θ. That is why the radius of the island base r, the perimeter of circle l, the surface area S, and the volume V can be expressed in terms of R_C: $r = R_C \sin\theta$, $l = 2\pi R_C \sin\theta$, $S = 4\pi R_C^2 \alpha_2(\theta)$, $V = \frac{4}{3}\pi R_C^3 \alpha_1(\theta)$, where $\alpha_1(\theta) = \frac{2-3\cos\theta+\cos^2\theta}{4}$, $\alpha_2(\theta) = \frac{1-\cos\theta}{2}$ [36].

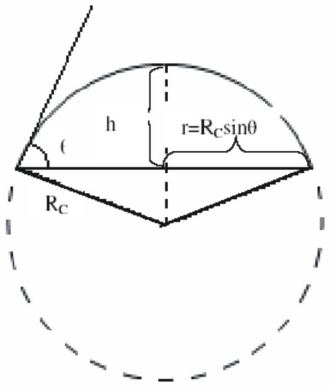

Fig. 1. Island (cluster) in the form of a spherical segment being a part of the sphere with the radius R_C

The concentration of adatoms near the base of clusters C_r is given by the Gibbs–Thomson formula

$$C_r = C_\infty e^{\Delta P \frac{\upsilon_m}{kT}} \approx C_\infty \left(1 + \Delta P \frac{\upsilon_m}{kT}\right), \quad (1)$$

where C_∞ denotes the equilibrium concentration at the temperature T, υ_m is the adatom volume, k is the Boltzmann constant, and ΔP stands for the Laplace pressure caused by the surface curvature of an island. It can be determined by equating the work required for a decrease of the island volume by dv to the reduction of the free energy of the island surface caused by it:

$$\Delta P d\mathrm{v} = \sigma dS \;\; \text{або} \;\; \Delta P = \sigma \frac{dS}{d\mathrm{v}} = 2\frac{\sigma}{R_C}\frac{\alpha_2(\theta)}{\alpha_1(\theta)}, \quad (2)$$

where σ is the specific value of the surface energy.

With regard for (2), formula (1) can be rewritten as

$$C_r = C_\infty e^{\frac{2\sigma}{R_C}\frac{\upsilon_m}{kT}\frac{\alpha_2(\theta)}{\alpha_1(\theta)}} = C_\infty e^{\frac{2\sigma}{r}\frac{\upsilon_m \sin\theta}{kT}\frac{\alpha_2(\theta)}{\alpha_1(\theta)}} =$$

$$= C_\infty \left(1 + \frac{2\sigma}{r}\frac{\upsilon_m \sin\theta}{kT}\frac{\alpha_2(\theta)}{\alpha_1(\theta)}\right). \quad (3)$$

It is worth noting that the Gibbs–Thomson formula in the form (3) is presented for the first time.

Thus, the concentration of adatoms at the "cluster—substrate" interface along the boundary line (along the perimeter of the cluster) is determined by the curvature radius of the cluster base r, exactly as it should be for a plane problem. The smaller the cluster radius r, the larger must be the concentration of adatoms at the interface. *Vice versa*, the higher the cluster radius, the lower C_r. On the substrate, some average concentration $\langle C\rangle$ determined by the critical radius r_k is established:

$$\langle C\rangle = C_\infty e^{\frac{2\sigma}{r_k}\frac{\sin\theta}{kT}\frac{\alpha_2(\theta)}{\alpha_1(\theta)}} \approx C_\infty \left(1 + \frac{2\sigma}{r_k}\frac{\sin\theta}{kT}\frac{\alpha_2(\theta)}{\alpha_1(\theta)}\right). \quad (4)$$

The clusters, for which $C_r > \langle C\rangle$, will dissolve. The clusters, for which $C_r < \langle C\rangle$, will grow. Those clusters of critical size, whose radius is determined by Eq. (4), are in equilibrium with the solution of adatoms:

$$r_k = \frac{\alpha}{\Delta}, \quad (5)$$

where $\alpha = \frac{2\sigma C_\infty \upsilon_m}{kT}\sin\theta\frac{\alpha_2(\theta)}{\alpha_1(\theta)}$, the oversaturation $\Delta = \langle C\rangle - C_\infty$.

In the case of the diffusion mechanism of growth of dome-shaped clusters, the mass transfer between them is realized by the surface diffusion under conditions of a self-consistent diffusion field [37,38] characterized by the surface diffusion coefficient D_S. Reaching the perimeter of islands due to the surface diffusion and overcoming the potential barrier at the "island–substrate" interface, adatoms get to their surface. The redistribution of adatoms over the surface of clusters is implemented by capillary forces (surface tension forces).

According to the Wagner theory, the surface mechanism of growth with conservation of the form of islands, i.e. with conservation of the contact angle θ, is realized if atoms, that cross the "island–substrate" interface and get to the island surface for unit time, have time to form chemical bonds necessary for the reconstruction of the structure of the island substance. Otherwise, there takes place the accumulation of adatoms around the "island–substrate" interface with the concentration C equal to the average concentration of the solution $\langle C\rangle$. In this case, the process of growth is already controlled by the kinetic coefficient β rather than by the surface diffusion coefficient D_S.

In accordance with the Wagner theory, the number of adatoms that cross the "island–substrate" interface and get to the island surface for unit time is

$$j_1 = 4\pi R_C \alpha_2(\theta)\beta\langle C\rangle = 4\pi r^2 \frac{\alpha_2(\theta)}{\sin^2\theta}\beta\langle C\rangle, \quad (6)$$

while the number of atoms that leave it for unit time is

$$j_2 = 4\pi r^2 \frac{\alpha_2(\theta)}{\sin^2\theta}\beta C_r, \quad (7)$$

so that the summary flow of atoms taking part in the formation of chemical bonds is equal to

$$j_i = j_1 - j_2 = 4\pi r^2 \frac{\alpha_2(\theta)}{\sin^2\theta}\beta\left(\langle C\rangle - C_r\right), \quad (8)$$

where C_r is specified by formula (3).

At the same time, the diffusion flow of adatoms j_S to the island (from an island) is determined by the concentration gradient $\left(\frac{dC}{dR}\right)_{R=r}$ at the "island–substrate" interface:

$$j_S = 2\pi r D_S \left(\frac{dC}{dR}\right)_{R=r}. \quad (9)$$

It can be found by solving Fick's equation that describes the concentration of adatoms near a separate island and takes the following form under the conditions of stationarity and radial symmetry:

$$\frac{1}{R}\frac{d}{dR}\left(RD_S\frac{dC}{dR}\right) = 0. \quad (10)$$

Here, R varies within the limits $r \le R \le lr$, $l = 2,\ 3$ (screening distance [35]).

The solution of (10) can be presented as

$$C(R) = C_1 \ln \frac{R}{r} + C_2, \tag{11}$$

where the constants C_1 and C_2 are determined from the boundary conditions

$$C(R) = C_r, \quad \text{if} \quad R = r \tag{12}$$

$$C(R) = \langle C \rangle, \quad \text{if} \quad R = lr, \tag{13}$$

so that

$$C_1 = \frac{\langle C \rangle - C_r}{\ln l}, \quad C_2 = C_r. \tag{14}$$

Thus, the solution of (11) will have the form

$$C(R) = \frac{\langle C \rangle - C_r}{\ln l} \ln \frac{R}{r} + C_r. \tag{15}$$

Knowing $C(R)$, we obtain

$$j_S = \frac{2\pi D_S}{\ln l} \left(\langle C \rangle - C_r \right). \tag{16}$$

In the equilibrium state,

$$j_i = j_S = j. \tag{17}$$

That is why the flow j to the cluster (from a cluster) can be expressed as $j = \frac{1}{2}(j_i + j_S)$ and, in the general case,

$$j = (j_i + j_S). \tag{18}$$

The aim of the given work lies in the calculation of the size distribution function of islands (clusters, particles) and the corresponding time dependences for the average $\langle r \rangle$ (critical) and maximal dimensions of islands depending on the relation between the flows j_S and j_i.

2. Growth Rate of Islands

In order to determine the island size distribution function $f(r, t)$, it is necessary to know their growth rate $\dot{r} = \frac{dr}{dt}$ as they are linked with each other by the continuity equation

$$\frac{\partial f(r,\ t)}{\partial t} + \frac{\partial}{\partial t} \left[f(r,\ t)\, \dot{r} \right] = 0. \tag{19}$$

The growth rate of a separate island is determined from the condition

$$\frac{d}{dt} \left(\frac{4}{3} \pi R_C^3 \alpha_1(\theta) \right) = \frac{d}{dt} \left(\frac{4}{3} \pi \frac{r^3}{\sin^3 \theta} \alpha_1(\theta) \right) = j \upsilon_m, \tag{20}$$

where j is specified by Eq. (18).

With regard for (8) and (16), we can obtain the growth rate of islands from (20) as

$$\frac{dr}{dt} = \frac{1}{4\pi r^2} \frac{\sin^3 \theta}{\alpha_1(\theta)} \upsilon_m \times$$

$$\times \left[4\pi r^2 \frac{\alpha_2(\theta)}{\sin^2(\theta)} \beta \left(\langle C \rangle - C_r \right) + \frac{2\pi D_S}{\ln l} \left(\langle C \rangle - C_r \right) \right]. \tag{21}$$

We denote the ratio of the flows by

$$\frac{j_S}{j_i} = \frac{x}{1-x}, \tag{22}$$

where $x = \frac{j_S}{j}$ is the contribution of the flow j_S to the summary flow j, and, respectively, $(1-x) = \frac{j_i}{j}$.

In order to express the growth rate (21) in terms of the flows j_i and j_S, we factor out the second term $\frac{2\pi D_S}{\ln l} \left(\langle C \rangle - C_r \right)$ and multiply the numerator and the denominator of the first term by $\left(\langle C \rangle - C_{r_g} \right) r_g^2$, where C_{r_g} is the concentration of adatoms at the interface of an island of the maximal size r_g:

$$\frac{dr}{dt} = \frac{1}{4\pi r^2} \frac{\sin^3 \theta}{\alpha_1(\theta)} \left(\langle C \rangle - C_r \right) \frac{2\pi D_S}{\ln l} \upsilon_m \times$$

$$\times \left[\frac{4\pi r_g^2 \frac{\alpha_2(\theta)}{\sin^2 \theta} \beta \left(\langle C \rangle - C_{r_g} \right) \frac{r^2}{r_g^2}}{\frac{2\pi D_S}{\ln l} \left(\langle C \rangle - C_{r_g} \right)} + 1 \right]. \tag{23}$$

The first term in the square brackets is equal to the ratio of the flows j_i / j_S for a particle of the maximal size. According to relation (22), it can be replaced by $\frac{1-x}{x}$, because expression (22) does not impose any restrictions on the particle size. In addition, in view of the relation

$$\langle C \rangle - C_r = \frac{2\sigma C_\infty \upsilon_m}{kT} \sin\theta \frac{\alpha_2(\theta)}{\alpha_1(\theta)} \left(\frac{1}{r_k} - \frac{1}{r} \right),$$

formula (23) for the growth rate can be rewritten as

$$\frac{dr}{dt} = \frac{\sigma C_\infty \upsilon_m^2 D_S}{kT} \frac{\sin^4 \theta \alpha_2(\theta)}{\alpha_1^2(\theta) \ln l} \frac{1}{r^3} \left(\frac{1-x}{x} \frac{r^2}{r_g^2} + 1 \right) \times$$

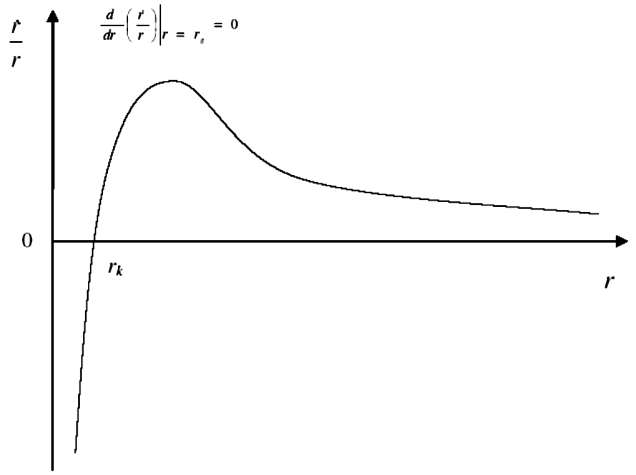

Fig. 2. Schematic dependence of the specific growth rate $\frac{\dot r}{r}$ on r

$$\times\left(\frac{r}{r_k}-1\right)=\frac{A^*}{r^3}\left(\frac{1-x}{x}\frac{r^2}{r_g^2}+1\right)\left(\frac{r}{r_k}-1\right), \qquad (24)$$

where $A^*=\frac{\sigma C_\infty v_m^2 D_S}{kT}\frac{\sin^4\theta\alpha_2(\theta)}{\alpha_1^2(\theta)\ln l}$.

Equation (24) determines the growth rate of islands under the conditions of surface diffusion with the contribution of the $(1-x)$-th part of the flow controlled by the kinetic coefficient β.

At $x=1$, Eq. (24) becomes

$$\frac{dr}{dt}=\frac{A^*}{r^3}\left(\frac{r}{r_k}-1\right) \qquad (25)$$

and coincides with formula (17 in [35].

Repeating the previous computations and factoring out $4\pi r^2\frac{\alpha_2(\theta)}{\sin^2\theta}\beta\left(\langle C\rangle-C_r\right)$, we obtain

$$\frac{dr}{dt}=\frac{2\sigma C_\infty v_m^2\beta}{kT}\frac{\sin^2\theta\alpha_2^2(\theta)}{\alpha_1(\theta)}\frac{1}{r}\left(\frac{x}{1-x}\frac{r_g^2}{r^2}+1\right)\times$$

$$\times\left(\frac{r}{r_k}-1\right)=\frac{B^*}{r}\left(\frac{x}{1-x}\frac{r_g^2}{r^2}+1\right)\left(\frac{r}{r_k}-1\right), \qquad (26)$$

where $B^*=\frac{\sigma C_\infty v_m^2\beta}{kT}\frac{\sin^2\theta\alpha_2^2(\theta)}{\alpha_1(\theta)}$. At $x=0$, Eq.(26) takes the form

$$\frac{dr}{dt}=\frac{B^*}{r}\left(\frac{r}{r_k}-1\right) \qquad (27)$$

which coincides with relation 31 in [35] for the growth rate of islands controlled by the kinetic coefficient β.

Equation (26) describes the nondiffusive Wagner mechanism of growth of islands with the contribution x of surface diffusion.

3. Time Dependences of r_g and r_k

One of the basic parameters of the LSW theory is the parameter u_0 – the so-called locking point. In our case, it equals $u_0=r_g/r_k$. Using u_0 and Eq. (24) or (26) for the growth rate, we can not only find the time dependences for r_g and r_k but can also determine the analytic form of the size distribution function, by integrating the continuity equation after the separation of variables in it.

The value of u_0 is found from the equation for the specific growth rate (i.e. the growth rate per unit length of the island radius) rather than from the growth rate equation [11]. For example, with the use of (24), the specific growth rate can be written as

$$\frac{\dot r}{r}=\frac{A^*}{r^4}\left(\frac{1-x}{x}\frac{r^2}{r_g^2}+1\right)\left(\frac{r}{r_k}-1\right). \qquad (28)$$

The schematic dependence of $\dot r/r$ on r is presented in Fig. 2. At the point where $\dot r/r$ reaches a maximum, the derivative is equal to zero. From this condition, we get

$$\frac{d}{dr}\left(\frac{\dot r}{r}\right)\Big|_{r=r_g}=0 \qquad (29)$$

and

$$u_0=\frac{r_g}{r_k}=\frac{2x+2}{2x+1}. \qquad (30)$$

At $x=0$ (the Wagner mechanism of growth), $\frac{r_g}{r_k}=2$; at $x=1$ (the diffusion mechanism of growth), $\frac{r_g}{r_k}=\frac{4}{3}$.

Using the value of u_o (30), the specific growth rate (28) can be expressed in terms of the dimensionless variable $u=\frac{r}{r_g}$, which allows us to represent it graphically depending on the relation between the flows rather than schematically:

$$\upsilon'=\frac{r_g^4}{A^*}\frac{dr}{dt}=\frac{1}{u^4}\left(\frac{1-x}{x}u^2+1\right)\left(\frac{2x+2}{2x+1}u-1\right), \qquad (31)$$

where the dimensionless specific rate of growth $\upsilon'=\frac{r_g^4}{A^*}\frac{dr}{dt}$. Figure 3 shows the dependence of υ' on u for various x. The role of the locking point is defined by the fact that, within the framework of the LSW theory, all solutions including the size distribution function are determined only for the values of u_0.

In order to determine r_g and r_k, we use Eqs. (24) and (26). Substituting $r = r_g$ into (24), replacing the ratio $\frac{r_g}{r_k}$ by its value (30), and integrating, we obtain

$$r_g^4 = 4\frac{A^*}{x\,(2x+1)}t \tag{32}$$

or:

$$r_k^4 = 4A^*\frac{(2x+1)^3}{x\,(2x+2)^4}t. \tag{33}$$

At $x = 1$, the growth of islands is completely controlled by the surface diffusion coefficient [35]:

$$r_g^4 = \frac{4}{3}A^*t, \quad r_k^4 = \frac{27}{64}A^*t, \quad \frac{r_g}{r_k} = \frac{4}{3}. \tag{34}$$

Similarly, Eq. (26) gives

$$r_g^2 = 2\frac{B^*}{(1-x)\,(2x+1)}t, \quad r_k^2 = 2\frac{B^*\,(2x+1)}{(1-x)\,(2x+2)^2}t. \tag{35}$$

Equations (35) describe the growth of islands under the conditions controlled by the kinetic coefficient β with the contribution x of surface diffusion. If $x = 0$, then the growth process is completely controlled by the kinetics of the transition through the "island–substrate" interface [4]:

$$r_g^2 = 2B^*t, \quad r_k^2 = \frac{1}{2}B^*t, \quad \frac{r_g}{r_k} = 2. \tag{36}$$

4. Relative Size Distribution Function $g\,(u)$

According to [11], the size distribution function of clusters (islands) in the interval $0 \le x \le 1$ is presented in the form of the product

$$f\,(r,\ t) = \varphi\,(r_g)\,g'\,(u)\,, \tag{37}$$

where $g'\,(u)$ is the relative size distribution of clusters, $u = \frac{r}{r_g}$. The function $\varphi\,(r_g)$ is determined from the law of conservation of the dispersed phase volume:

$$\Phi = \frac{4}{3}\pi\alpha_1\,(\theta)\,\frac{1}{\sin^3\theta}\int\limits_0^{r_g} r^3 f\,(r,\ t)\,dr. \tag{38}$$

Substituting $f\,(r,\ t)$ from (37) into (38), we obtain

$$\varphi\,(r_g) = \frac{Q}{r_g^4}, \tag{39}$$

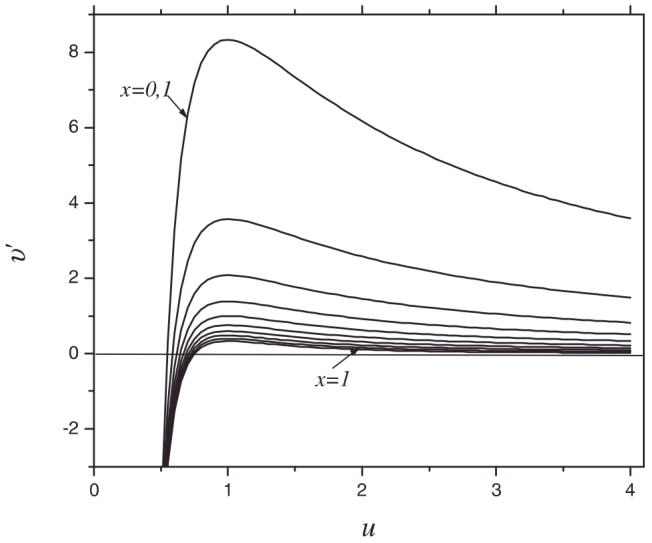

Fig. 3. Dependence of the dimensionless growth rate υ' on u for various x

where $Q = \frac{\Phi}{\frac{4}{3}\pi\alpha_1(\theta)\frac{1}{\sin^3\theta}\int\limits_0^1 u^3 g'(u)du} = \frac{\Phi'}{\int\limits_0^1 u^3 g'(u)du}$, $\Phi' = \frac{\Phi\sin^3\theta}{\frac{4}{3}\pi\alpha_1(\theta)}$. Taking (39) into account, $f\,(r,\ t)$ can be rewritten as

$$f\,(r,\ t) = \frac{g\,(u)}{r_g^4}, \tag{40}$$

where

$$g\,(u) = Qg'\,(u)\,. \tag{41}$$

In order to determine $g'\,(u)$, we use the continuity equation (19) by replacing $f\,(r,\ t)$ and $\dot r$ by their values from (40) and (26) (or (24)). In the case of the transition from the differentiation with respect to r and t to the differentiation with respect to u, the separation of variables takes place and (19) becomes

$$\frac{dg'\,(u)}{g'\,(u)} = -\frac{4\upsilon_g - \frac{1}{u}\frac{d\upsilon}{du} + \frac{\upsilon}{u^2}}{u\upsilon_g - \frac{\upsilon}{u}}du, \tag{42}$$

where

$$\upsilon = \frac{r\dot r}{B^*} = \left(1 + \frac{x}{1-x}\frac{1}{u^2}\right)\left(\frac{2x+2}{2x+1}u - 1\right),$$

$$\upsilon_g = \upsilon|_{u=1} = \frac{r_g}{B^*}\frac{dr_g}{dt} = \frac{1}{(1-x)\,(2x+1)},$$

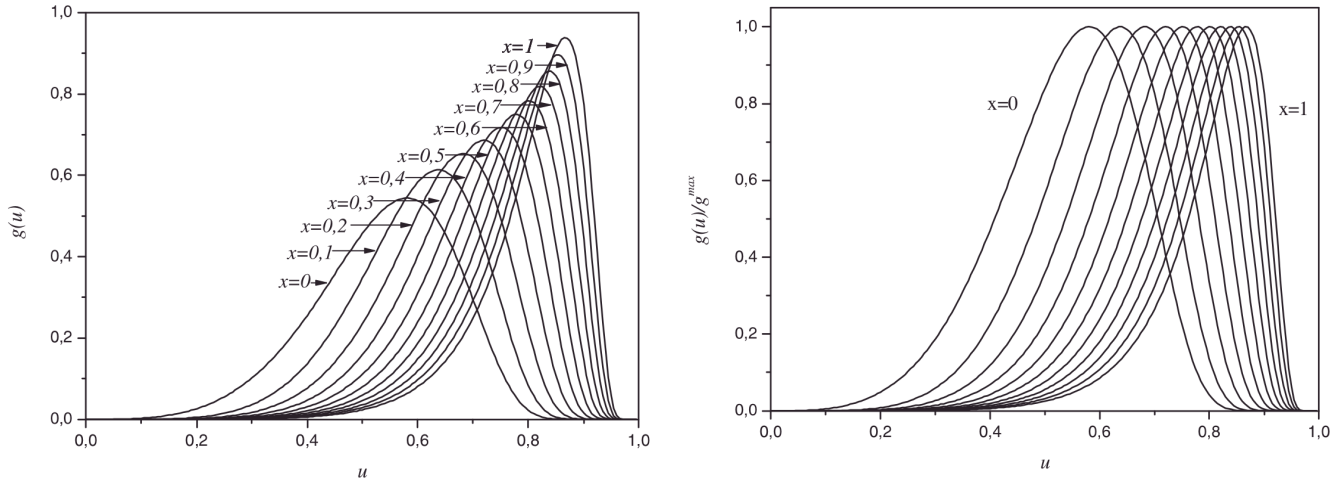

a **b**

Fig. 4. Function $g(u)$ calculated according to (47) (*a*) and $(g(u)/g^{max}$ (*b*)

$$\frac{du}{dr}=\frac{1}{r_g},\quad \frac{du}{dr_g}=-\frac{u}{r_g}.$$

Substituting υ, υ_g, and $\frac{d\upsilon}{du}$ into (42), we obtain the expression

$$\frac{dg'(u)}{g'(u)}=$$

$$=-\frac{4u^4-u^2\left(1+x-2x^2\right)+4u\left(x^2+x\right)-3x\left(2x+1\right)}{u\left(1-u\right)^2\left(u^2+2ux^2+2x^2+x\right)}du, \tag{43}$$

whose integration allows us to find

$$g'(u)=\frac{u^3\left(u^2+2ux^2+2x^2+x\right)^{D/2}}{\left(1-u\right)^B}\times$$

$$\times\exp\left(\frac{F-Dx^2}{\sqrt{2x^2+x-x^4}}\mathrm{arctg}\frac{u+x^2}{\sqrt{2x^2+x-x^4}}\right)\times$$

$$\times\exp\left(\frac{C}{1-u}\right), \tag{44}$$

where

$$B=\frac{32x^4+16x^3+48x^2+13x+5}{A},$$

$$C=-\frac{12x^2+3x+3}{A},$$

$$D=-\frac{80x^4+40x^3+15x^2+x+2}{A},$$

$$F=-\frac{32x^6+16x^5+54x^4+34x^3+8x^2}{A},$$

$$A=16x^4+8x^3+9x^2+2x+1.$$

At $x=0$, we obtain $B=5$, $C=-3$, $D=-2$, and $F=0$, and expression (44) corresponds to the Wagner distribution [4]:

$$g'(u)=u\left(1-u\right)^{-5}\exp\left(-\frac{3}{1-u}.\right). \tag{45}$$

At $x=1$, we obtain: $B=19/6$, $C=-1/2$, $D=-23/6$, $F=-4$ and expression (44) transforms into the Chakraverty distribution [35]:

$$g'(u)=\frac{u^3\exp\left(-\frac{1}{2(1-u)}\right)\exp\left(-\frac{1}{6\sqrt{2}}\mathrm{arctg}\frac{u+1}{\sqrt{2}}\right)}{\left(1-u\right)^{19/6}\left(u^2+2u+3\right)^{23/12}}. \tag{46}$$

With regard for the law of conservation of the volume (mass) of the island condensate, the relative size distribution function of clusters $g(u)$ can be found from Eq. (41) as

$$g(u)=\frac{g'(u)}{Q}. \tag{47}$$

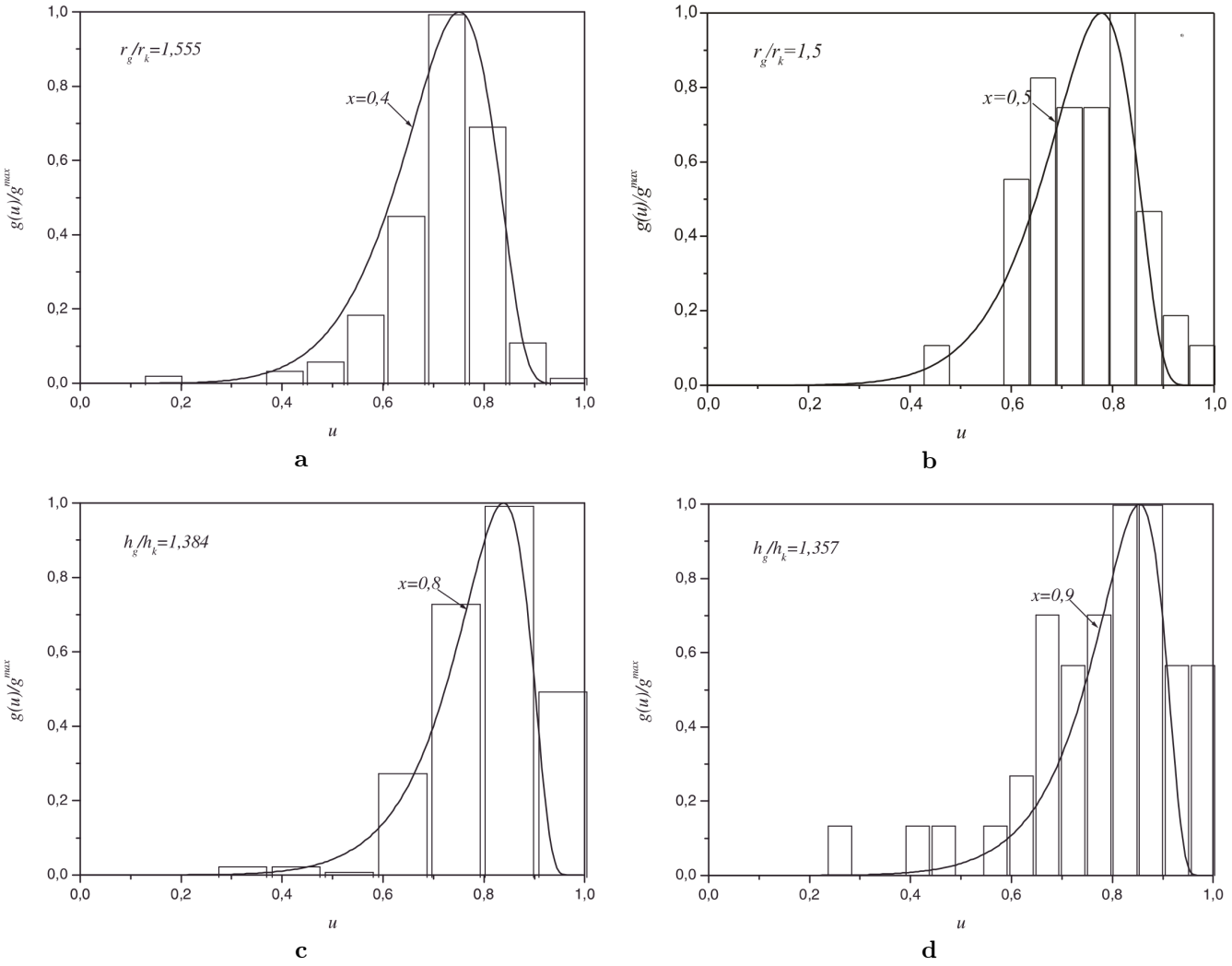

Fig. 5. Comparison of curve (47) with experimental diameter (d) and height (h) histograms of Mn nanopoints at various temperatures and thicknesses of Mn monolayers (ML): a – room temperature, Mn, 0.21 ML $\frac{r_g}{r_k} = 1.555$; b – 180 °C, $\frac{r_g}{r_k} = 1.5$; c – room temperature, Mn 0.21 ML $\frac{h_g}{h_k} = 1.384$; d – 180 °C, $\frac{h_g}{h_k} = 1.357$

5. Discussion

The curves presented in Fig. 4,a correspond to the calculated size distribution (47) at various values of x. The curves $x = 0$ and $x = 1$ correspond to the Wagner and Chakraverty distributions, respectively [4,35]. All the other curves in the range $0 < x < 1$ describe the island size distribution in the case of the simultaneous action of the Wagner and diffusion mechanisms of growth of clusters.

The same curves normalized to their maxima are presented in Fig. 4,b. In such a form normalized to unity with respect to the coordinate axes, they can be easily compared with the experimental histograms.

For the calculated family of distributions (47), the value of the locking point changes according to (30) in the range $2 \leq u_0 \leq 4/3$. At $x = 0.5$, $u_0 = \frac{3}{2}$, which coincides with the analogous value for the Lifshitz–Slyozov distribution. At the same time, curve (47) at $x = 0.5$ doesn't represent the Lifshitz–Slyozov distribution:

$$g(u) =$$

$$= \left\{ u^3 \exp\left[-1.084435 \operatorname{arctg}\left(1.032795u + 0.258199\right)\right] \times \right.$$

$$\left. \times \exp\left(-\frac{1.2}{1-u}\right) \right\} \Big/ \left\{ (1-u)^{22/5} \left(u^2 + 0,5u + 1\right)^{4/3} \right\}.$$

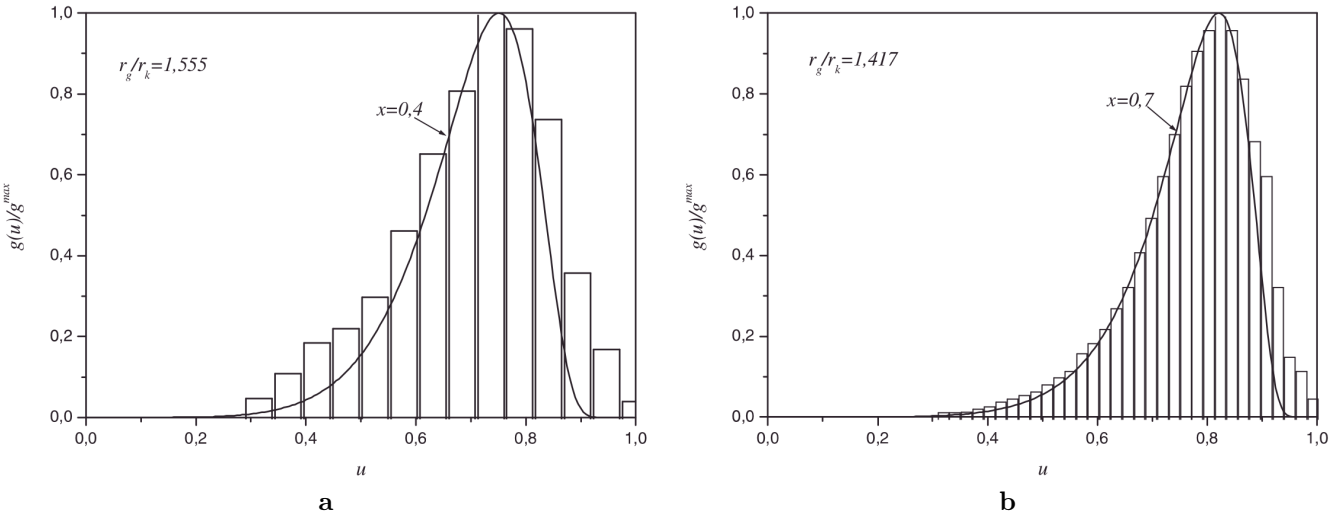

a **b**

Fig. 6. Comparison of curve (47) with experimental histograms of Au particles obtained using the method of molecular-beam epitaxy at the temperature of 525 °C (*a*) and after the 180-min isothermal exposure (*b*)

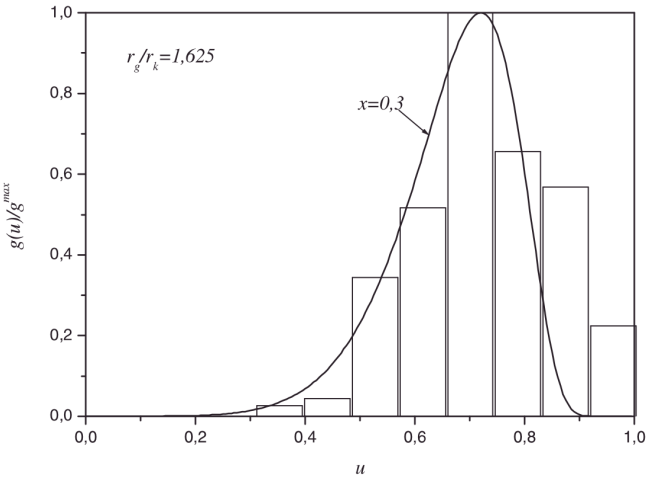

Fig. 7. Comparison of curve (47) with the experimental histogram of Ag nanoclusters obtained using the method of molecular-beam epitaxy at room temperature on a $TiO_2(110)$ substrate

This means that one cannot judge the character of a distribution by the value of the locking point u_0. It can serve as an estimating parameter when choosing a theoretical curve from family (47) for the sake of comparison to a necessary experimental histogram.

Another important peculiarity of the calculated distribution (47) lies in the fact that it can be used not only for comparison to experimental histograms in the form of the radial (r) distribution of particles but also for description of their height (h) distribution. One can see from Fig. 1 that the height of an island is equal to

$$h = R_C\,(1 - \cos\theta) = r\frac{1 - \cos\theta}{\sin\theta},$$

so that the ratio $\frac{r}{r_g} = \frac{h}{h_g} = u$.

Figure 5 shows the comparison of the theoretical curve (47) with the experimental diameter (a and b) and height (c and d) histograms of Mn nanopoints on a Si substrate obtained with the help of the method of molecular-beam epitaxy at various temperatures: room one (a, c) and a temperature of 180 °C (b, d) as well as at various thicknesses of Mn molecular layers (ML) [39]. The results of the comparison demonstrate that, in the case of the experimental diameter distributions, the contribution of each of the growth mechanisms (Wagner and diffusion ones) are approximately equal: Fig. 5,*a*, $x = 0.4$; Fig. 5,*b*, $x = 0.5$. At the same time, in the case of the height distributions, the diffusion growth mechanism prevails: Fig. 5,*c*, $x = 0.8$; Fig. 5,*d*, $x = 0.9$. This means that, in the process of growth, the height dimension of Mn nanopoints surpasses the lateral dimension d, so that $\frac{h}{d} > 1$. Possibly, this fact explains the form of Mn nanopoints obtained in [39].

In Fig. 6, one can see the results of comparison of the theoretical curve (47) with the experimental histograms of gold particles obtained at a temperature of 525 °C on a silicon substrate (Au/Si(111)) (*a*) and after the 180-min isothermal exposure (*b*) [40]. Judging by the value of x, the growth of particles is controlled at the beginning (Fig. 6,*a*) by the kinetic coefficient β. However, the mechanism of growth changes with time and, after a three-hour exposure, becomes mainly diffusive (Fig. 6,*b*).

The proposed growth mechanism is also confirmed by the results of comparison of the theoretical curve

calculated at $x = 0.3$ with the experimental histogram of Ag nanoclusters obtained with the help of the method of molecular-beam epitaxy at room temperature on a $TiO_2(110)$ substrate [41] (Fig. 7).

The considered examples of comparison of the calculated and experimental data allow us to make a conclusion about the possibility of a practical realization of the simultaneous action of two growth mechanisms – Wagner and diffusion ones. Moreover, such a situation where two growth mechanisms act simultaneously is possibly more general than the manifestation of one of them earlier considered separately by Wagner and Chakraverty.

1. W. Ostwald, Zs. Phys. Chem. **34**, 495 (1900).
2. I.M. Lifshits and V.V. Slyozov, Zh. Eksp. Teor. Fiz. **35**, 479 (1958).
3. I.M. Lifshits and V.V. Slyozov, J. Phys. Chem. Solids **19**, 35 (1961).
4. C. Wagner, Zs. Electrochem. **65**, 581 (1961).
5. R.D. Vengrenovich, B.V. Ivanskii, and A.V. Moskalyuk, Zh. Eksp. Teor. Fiz. **131**, 1040 (2007).
6. V.V. Slyozov, Fiz. Tverd. Tela **9**, 1187 (1967).
7. H.O.K. Kirchner, Metall. Trans. **2**, 2861 (1971).
8. H. Kreye, Zs. Metallkunde, **61**, 108 (1970).
9. A.J. Ardell, Acta Metall. **20**, 602 (1972).
10. R.D. Vengrenovich, Fiz. Met. Metaloved. **39**, 435 (1975).
11. R.D. Vengrenovich, Acta Metal. **30**, 1079 (1982).
12. R.D. Vengrenovich, Yu.V. Gudyma, and S.V. Yarema, Fiz. Met. Metaloved. **91**, 16 (2001).
13. R.D. Vengrenovich, Yu.V. Gudyma, and S.V. Yarema, Scripta Materialia **46**, 363 (2002).
14. R.D. Vengrenovich and Yu.V. Gudyma, Fiz. Tverd. Tela **43**, 1171 (2001).
15. R.D. Vengrenovich, Yu.V. Gudyma, and D.D. Nikirsa, J. Phys.: Condens. Matter. **13**, 2947 (2001).
16. A.P. Alekhin, Usp. Sovr. Radioelektr. **5**, 118 (2004).
17. M.S. Dunaevskii, Z.F. Krasil'nik, D.N. Lobanov, A.V. Novikov, A.N. Titkov, and R. Laiho, Fiz. Tekhn. Polupr. **37**, 692 (2003).
18. R.A. Andrievskii, Ros. Khim. Zh. **46**, 50 (2002).
19. V.F. Reutov and S.N. Dmitriev, Ros. Khim. Zh. **46**, 74 (2002).
20. M. Roko, Ros. Khim. Zh. **46**, 90 (2002).
21. N.N. Gerasimenko, Ros. Khim. Zh. **46**, 30 (2002).
22. S.M. Alfimov, V.A. Bykov, E.P. Grebennikov, S.I. Zheludeva, P.P. Mal'tsev, V.F. Petrunin, and Yu.A. Chaplygin, Mikrosist. Tekhn. **8**, 2 (2004).
23. M.C. Bartelt and J.W. Evans, Phys. Rev. B **46**, 12675 (1992).
24. N.C. Bartelt, W. Theis, and R.M. Tromp, Phys. Rev. B **54**, 11741 (1996).
25. M.I. Goldfarb, P.T. Hayden, J.H.G. Owen, and G.A.D. Briggs, Phys. Rev. Lett. **78**, 3959 (1997); Phys. Rev. B **56**, 10459 (1997).
26. B.A. Joyce, D.D. Vvedensky, A.R. Avery, J.G. Belk, H.T. Dobbs, and T.S. Jones, Appl. Surf. Sci. **130–132**, 357 (1998).
27. T.I. Kamins, G. Medeiros-Ribeiro, D.A.A. Ohlberg, and R.S. Williams, J. Appl. Phys. **85**, 1159 (1999).
28. R.D. Vengrenovich, Yu.V. Gudyma, and S.V. Yarema, Fiz. Tekhn. Polupr. **35**, 1440 (2001).
29. R.D. Vengrenovich, Yu.V. Gudyma, and S.V. Yarema, Phys. Stat. Sol. (B) **242**, 881 (2005).
30. O.P. Pchelyakov, Yu.B. Nikiforov, A.I. Yakimov, and B. Voightlander, Fiz. Tekhn. Polupr. **34**, 1281 (2000).
31. N.N. Ledentsov, V.M. Ustinov, V.A. Shchukin *et. al.*, Fiz. Tekhn. Polupr. **32**, 385 (1998).
32. R.D. Vengrenovich, A.V. Moskalyuk, and S.V. Yarema, Fiz. Tverd. Tela **49**, 13 (2007).
33. R.D. Vengrenovich, A.V. Moskalyuk, and S.V. Yarema, Fiz. Tekhn. Polupr. **40**, 276 (2006).
34. R.D. Vengrenovich, A.V. Moskalyuk, and S.V. Yarema, Ukr. J. Phys. **51**, 307 (2006).
35. B.K. Chakraverty, J. Phys. Chem. Solids **28**, 2401 (1967).
36. J.P. Hirth and G.M. Pound, *Condensation and Evaporation* (Pergamon Press, Oxford, 1963).
37. V.V. Slyozov and V.V. Sagalovich, Usp. Fiz. Nauk **151**, 67 (1987).
38. S.A. Kukushkin and A.V. Osipov, Usp. Fiz. Nauk **168**, 1083 (1998).
39. De-yong Wang, Li-jun Chen, Wei He, Qing-feng Zhan, and Zhao-hua Cheng, J. Phys. D: Appl. Phys. **39(2)**, 347 (2006).
40. P. Werner, N.D. Zakharov, G. Gerth, L. Schubert, and U. Gosele, Int. J. Mat. Res. (formerly Z. Metallkd.) **97**, 7 (2006).
41. Xiaofeng Lai, Todd P. St.Clair and D. Wayne Goodma, Faraday Discuss. **114**, 279 (1999).

Received 17.03.08

УЗАГАЛЬНЕНИЙ РОЗПОДІЛ ЧАКРАВЕРТІ–ВАГНЕРА

Р.Д. Венгренович, Б.В. Іванський, А.В. Москалюк

Р е з ю м е

Запропоновано механізм оствальдівського дозрівання острівців у тонких плівках і гетероструктурах в умовах одночасної дії дифузійного і вагнерівського механізмів росту. Розраховано функцію розподілу острівців за розмірами і відповідні їй часові залежності для середніх (критичних) та максимальних розмірів острівців. Зіставлення експериментальних гістограм з розрахованими кривими підтверджує можливість реалізації на практиці запропонованого механізму росту у процесі оствальдівського дозрівання.